Chapter 6
Characteristics of Carbon Nanotubes

Soma Banerjee and Kamal K. Kar

Abstract Carbon nanotubes (CNTs) are the materials of modern age having diverse applications in every sector. This article discusses the structure, synthesis, properties, purification, and application aspects of CNTs. CNTs can be classified based on tube structure and shapes. This chapter elaborates single-walled nanotubes (SWNTs), multi-walled nanotubes (MWNTs), and double-walled nanotubes (DWNTs) in brief. In addition, researches are going on worldwide to generate CNTs of variable shapes such as coiled, waved, bent, beaded, junction CNTs. CNTs can be synthesized by chemical and physical routes. The most common method of CNT production is chemical vapour deposition (CVD) technique that can produce pure CNTs in large quantities. This article also opens up the present aspects of growth mechanism of CNTs. The unique combination of electrical, thermal, and mechanical properties of CNTs makes them a potential performer in the number of fields such as supercapacitors, fuel cells, energy devices, high strength composites, biomedical, chemical. However, the application of CNTs is still somehow limited and yet to reach the desired plateau due to the purification, large-scale production, and toxicity issues.

6.1 Introduction

Since prehistoric times, carbon has been used in different forms in various aspects of art and technology [1–3]. Starting from the use of charcoal and soot in cave paintings to modern use of carbon nanomaterials, carbon has a remarkable impression in every

S. Banerjee · K. K. Kar (✉)
Advanced Nanoengineering Materials Laboratory, Materials Science Programme, Indian Institute of Technology Kanpur, Kanpur 208016, India
e-mail: kamalkk@iitk.ac.in

S. Banerjee
e-mail: somabanerjee27@gmail.com

K. K. Kar
Advanced Nanoengineering Materials Laboratory, Department of Mechanical Engineering, Indian Institute of Technology Kanpur, Kanpur 208016, India

K. K. Kar (ed.), *Handbook of Nanocomposite Supercapacitor Materials I*,
Springer Series in Materials Science 300,
https://doi.org/10.1007/978-3-030-43009-2_6

sphere of life. The use of other forms of carbon such as graphite, carbon black, and charcoal is extensive in the field of drawing, writing, printing, etc. Charcoal has played a tremendous role in the first technology of human being, i.e. smelting and working of metals. Later on, in the advanced stage of eighteenth century, charcoal has been replaced by coke, which lead to an industrial revolution. In 1896, the first synthetic graphite has been synthesized by American Edward Acheson. Afterward in the twentieth century, and activated carbon has grabbed the attention due to the ability to purify waste water. The invention of carbon fiber in 1950s opens up the development of an interesting lightweight and ultra-strong carbon material to the engineers. Diamonds are industrially explored at around 1950s by the development of successful synthesis methodology by General Electrics. In 1980s, the research in the field of carbon science became mature and grabbed Nobel Prizes. In 1985, Harry Kroto and group have invented the first all carbon-based molecules named as buckminsterfullerene [4]. This development in carbon science opened up further synthesis of fullerene-related nanotubes.

In the year 1991, Ijima discovered the magical carbon nanomaterial, carbon nanotubes (CNTs) containing more than one graphitic layer having an inner diameter of 4 nm. In 1993, Bethune et al. and Ijima et al. have independently reported the development of single-walled nanotube (SWNT) [5, 6]. The discovery of SWNTs is remarkable since their structures are seemed to be close to theoretical prediction. The extraordinary properties of SWNTs have grabbed more attention the researcher compared to multi-walled nanotube (MWNTs). CNTs are tube-shaped carbon materials having a diameter in nanometres. The graphitic layers of CNTs are rolled-up chicken wire having carbon at the apex of a hexagon also called graphene. CNTs made of same graphite sheets can have different properties due to the difference in length, helicity, thickness, and number of layers, etc. Depending on the structural arrangements, they can be metallic or semiconductor in nature. MWNTs are CNTs composed of many graphitic shells having adjacent shell separation of 0.34 nm and diameter of 1 nm. Lengths of the nanotubes are of several microns and graphene sheets can be rolled in a number of ways generating different types of nanotube based on their structural arrangements. The high length-to-diameter ratio of these materials provides an interesting combination of properties catching the attention of researchers of interdisciplinary fields. The spatial arrangement of carbon atoms generates various carbon networks [7, 8]. Figure 6.1 represents different forms of carbon nanomaterials.

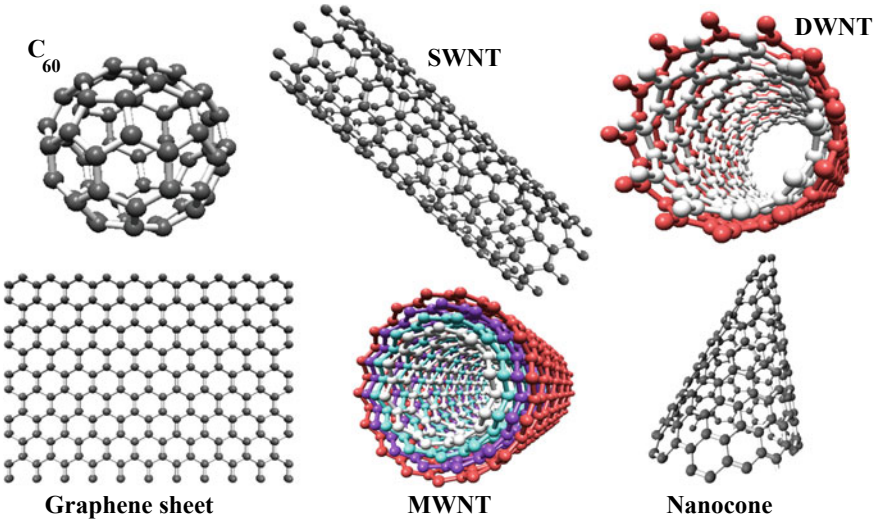

Fig. 6.1 Different forms of carbon nanomaterials

6.2 Structure of Carbon Nanotubes

6.2.1 Based on Tube Structure

6.2.1.1 Single-Walled Nanotubes

Single-walled nanotube (SWNT) can be imagined as a perfect graphene sheet consisting of sp^2 hybridized carbon in a hexagon, which is rolled in the form of a cylinder with the confirmation that the hexagonal rings located in contact are combined coherently. The tips of the tube are closed by a cap made of hemifullerene of a specific diameter. Single-walled nanotubes (SWNTs) are the nanomaterial of unique properties and behavior and a beautiful material for fundamental physicists and experimental chemists. Geometrically, the SWNT tube diameter can be anything; however, calculations reveal that the SWNT collapses into flatten ribbon-like structure and energetically the ribbon-like structure becomes more favourable once the diameter of the tube reaches 2.5 nm [9]. SWNTs of diameter as low as 0.4 nm have been reported [10]. For the tube length of SWNT, no such restriction is known; however, the length of the tubes will be governed by the method of synthesis and parameters of synthesis such as thermal gradient, residence time. The length of the SWNTs can be a few micrometres to millimetre range. These specific features of SWNT makes them a material of choice due to huge aspect ratio. A simple way of rolling of graphene sheet to form CNT is shown in Fig. 6.2.

From the structure of SWNTs, two different aspects can be discussed. First, all the carbons are a part of hexagonal rings and are in equivalent positions except at

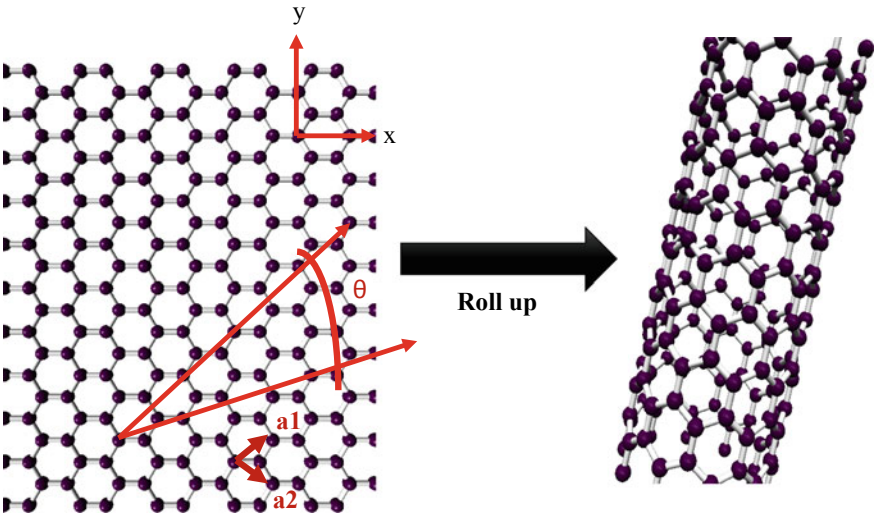

Fig. 6.2 Rolling up of graphene sheet to form nanotube. Drawn based on the concept taken from [11]

the tip of the nanotubes, where ($6 \times 5 = 30$) atoms of carbons are present forming pentagonal rings. Hence, for ideal cases, the reactivity will be exceptional at the tip part of the tube rather at the hexagonal part of it. Again, the carbon atoms in the aromatic ring are not exactly planar indicating the fact that the carbon atoms are not having pure sp^2 hybridization. There remains some sp^3 character as well, and this will be dependent on the radius of curvature of the tube. As for example, fullerenes C60 molecule having radius of curvature 0.35 nm possesses 10% sp^3 character [12]. These structural features make SWNT different from graphene, and SWNT is expected to have a bit more reactivity compared to planar graphene. These factors are again responsible for the overlapping of bands, and hence, a unique electrical behavior has been evidenced for SWNTs.

As discussed earlier, the graphene sheets can be rolled in a number of ways to form SWNTs giving rise to the formation of Zigzag, armchair, and helical SWNTs as represented in Fig. 6.3. Some of the nanotubes will possess planes of symmetry both perpendicular and parallel to the tube axis, while others will not. The latter is commonly named as chiral nanotubes since they are not able to superimpose on their mirror image. The way to roll a graphene sheet is mathematically expressed by the vector of helicity, C_h (OA), and angle of helicity, θ; i.e.,

$$OA = C_h = na_1 + ma_2 \tag{6.1}$$

where

$$a_1 = ax\sqrt{3}/2 + ay/2 \tag{6.2}$$

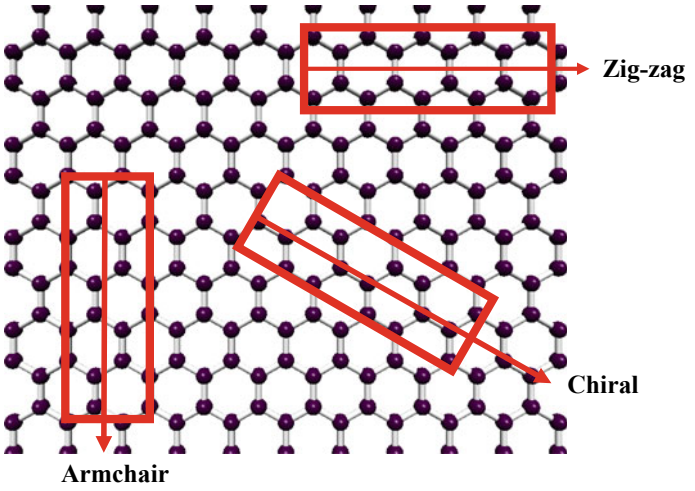

Fig. 6.3 SWNT structures of different types: zigzag, armchair, and helical nanotube. Drawn based on the concept taken from [14]

and

$$a_2 = ax\sqrt{3}/2 - ay/2 \tag{6.3}$$

where $a = 2.46$ Å
and

$$\cos\theta = (2n + m)/2\sqrt{(n^2 + m^2 + nm)} \tag{6.4}$$

The vector of helicity is considered as perpendicular to the nanotube axis, whereas the angle of helicity is taken at the zigzag axis. Hence, the zigzag type nanotubes are emerged due to the vector of helicity. The diameter (D) of a SWNT is related to C_h by the following equation.

$$\begin{aligned} D &= |C_h|/\pi = a_{C=C}\sqrt{3(n^2 + m^2 + nm)}/\pi \\ &1.41\ \text{Å} \le a_{C=C} \le 1.44\ \text{Å} \\ &\text{(graphite)} \quad (C_{60}) \end{aligned} \tag{6.5}$$

The parameters of helicity, C_h, θ, and tube diameter all are expressed as a function of integer values n and m. Hence, SWNT nomenclature is given as per the integer values as (n, m). The integer value, in other words, the naming of SWNT, can be easily given by calculating the number of hexagons separating the edges of C_h vector following a_1 and a_2 [13]. In general, it can be concluded that when the vector of helicity remains perpendicular to any of the three C=C bond directions, it generates

zigzag type SWNTs. On the other hand, when the vector of helicity remains parallel to C=C bond directions, it generates armchair types nanotubes denoted as (n, n).

6.2.1.2 Multi-walled Nanotubes

Multi-walled nanotube (MWNT) can be imagined as concentric carbon nanotube composed of many SWNTs of increasing diameter arranged coaxially as per the Russian doll model. These types of nanotubes are synthesized by electric arc method without the use of a catalyst or bycatalyst-assisted thermal cracking of gaseous hydrocarbons or by CO disproportionation reactions. The number of tubes can be in any numbers starting from two. The inter-tube distance is the same as that of the intergraphene distance of 0.34 nm a little more compared to the graphite of 0.335 nm. An increased radius of curvature during the formation of MWNT restricts the regular arrangement of carbons as in graphite. MWNTs can also be of faceted morphologies developed by thermal treatment at a very high temperature of around 2500 °C. Another common structural feature of MWNT is herringbone texture. Here, graphene forms an angle with the axis of the carbon nanotubes. The angle formed will be dependent on processing conditions such as morphology of the catalyst, composition of the reaction environment, etc. The angle may be varied from zero to 90° leading to the change of nanotube morphology to nanofibers [15]. Catalyst-induced thermal cracking of hydrocarbons and CO disproportionation is the common method used for the synthesis of herringbone MWNTs. The aspect ratio of MWNTs is small compared to SWNTs and often allows to predict tube ends when imaged under transmission electron microscopy. Again, imaging shows that the nanotube tips are associated with catalyst crystals when grown by the method of electric arc discharge.

A special attention is to be given to double-walled carbon nanotubes, abbreviated as DWNT having similar kinds of morphology and properties as that of SWNT with the additional benefit of improved chemical resistance properties. The synthesis of DWNT is proposed in 2003 by CCVD technique using selective reducing oxide solution in the presence of methane and hydrogen [16]. DWNTs can be modified more easily by the functionalization approach compared to SWNTs. In case of SWNTs, the functionalization leads to breaking of carbon–carbon double bonds creating holes in the structure of the nanotubes, which thereby leads to alteration in mechanical and electrical properties. For DWNTs, the outer walls are only modified by grafting of chemical entities at the nanotube surface to generate new properties in CNTs.

6.2.1.3 Nanotorus

The word nanotorus is theoretically explained as the CNTs made in the form of a doughnut, i.e., bent like a torus. These types of CNTs have extraordinary magnetic properties having 1000 times of magnetic moments. The radius of torus determines the magnetic moments and other properties of the doughnut such as thermal stability. These materials can be promising in nanophotonics [17].

6.2.1.4 Nanobuds

Carbon nanobuds can be defined as the new form of carbon made of two allotropes of carbon, namely CNT and fullerene. They are formed by covalent bonding between the CNTs and fullerenes. The fullerenes are bonded to the outer sidewalls of a CNT to form a bud over it. These materials are found to be excellent field emitters. The other utility of nanobuds is they can act like an anchor to matrix materials when used as a functional filler in the composites. The buds may prevent the slippage of CNTs inside the matrix of a composite, and hence, a remarkable improvement in mechanical properties can be achieved [18].

6.2.1.5 Nanohorns

Nanohorns are another interesting form of CNT discovered first by Haris and Ijima [19]. The single-walled nanohorn is defined as a horn-type SWNT with a conical tip [20]. The main utility of single-walled nanohorns is that they can be synthesized without catalysts and hence can be of very high purity. These materials are promising for energy storage applications and as an electrode material due to the high surface area and electronic properties. These materials have been extensively studied in other applications such as adsorption, gas storage, fuel cells, magnetic resonance analysis, catalyst supports, electrochemistry [21].

6.2.2 Based on Shapes

CNTs are studied extensively in recent days due to the provision to be tailored in a number of ways based on diameter, number of walls, tube length, crystallinity, purity, alignment, etc. [22, 23]. A perfect nanotube is composed of crystalline structure of hexagonal network. In the presence of defects, nanotubes get curved. The nanotubes of different morphologies have their potential in number of applications due to the unique variation in properties with shape. Till date, different shapes of CNTs are synthesized such as coiled, waved, branched, bent, beaded, straight.

6.2.2.1 Straight Carbon Nanotubes

Several methods generate vertically aligned CNTs by catalytic CVD [24]. The vertically aligned CNTs are the nanotubes that are oriented perpendicular to the substrate. Two major researches are to be mentioned for the development of CNT arrays—first by Fan et al. [25] and other by Hata et al. [26]. Fan et al. have developed blocks of MWNTs that have grown perpendicular to the substrate [25]. They have used porous silicon substrate with catalyst pattern via e-beam evaporation. Hata et al. have synthesized SWNT arrays of few millimetre height using water-assisted CVD technique

[26]. Study reveals that SWNT of DWNTs will collapse and generate stacks of parallel graphene layers when diameters become greater than 5 nm. Aligned CNT arrays are suitable in advanced devices such as light emitters, field-effect transistors, logic circuits, sensors [27–31].

6.2.2.2 Waved Carbon Nanotubes

A single nanotube generally bends during the process of growth if no external force is applied. The bends in nanotubes arise due to the presence of pentagon–heptagon defect pairs by means of local mechanical deformation forces. A nanotube can be elastically deformed by the application of small bending stress, and when the local curvature exceeds a critical value, it is buckled [31–33]. Again, when a nanotube grows, the interaction with other nanotubes may generate bending. In addition, limited growing space and its own weight can also be factors affecting the bending of a nanotube. This kind of regular bending may result in wavy-kind morphology in CNTs. Again, it is believed that wavy structures in nanotubes are generated when two types of catalysts are present over the substrate. One may be of higher catalytic activity than other leading to a high growth rate of CNTs. Due to the van der Walls forces, the nanotubes when touch each other stick together. The growth of CNT arrays is limited for catalyst present over the surface of the substrate with a relatively slow rate of growth. The nanotube growing at a higher rate is forced to bend. Hence, the extent of wavy nature will be dependent on the variation in the growth rate of these two groups. These kinds of structures of nanotubes are important for assembling of CNT sheets or yarns [34, 35].

6.2.2.3 Branched Carbon Nanotubes

Branched CNTs of the type *Y*-junction are formed by inserting non-hexagonal rings in a network of a hexagon in particular to the zones, where three arms of *Y* are clubbed together [36, 37]. Other structural arrangements of nanotubes also follow the same rule of protecting sp^2 hybridized carbon [38, 39]. The only difference lies in kind, placement, and number of non-hexagonal units. This opens up the provision of variation in angles from *Y* to *T* shapes [40, 41]. These structures have the potential for electrical applications since metallic and semiconducting tubes can be converted to CNT junctions for building different parts of nanometric-integrated circuits [42]. CNTs produced by the arc discharge process show *T*, *Y,* and *L* junctions [43]. Synthesis of most of the junctional CNTs is based on catalytic CVD [44–47]. Branched SWNTs have potential in advanced electronic devices such as nano-transistors, nano-interconnect, nano-diode [31].

6.2.2.4 Regularly Bent Carbon Nanotubes

Regular bends in CNTs are useful for their applications in the field of nanocircuit interconnects, high-resolution AFM tips, and many more. Nanotubes can be forced to be aligned during their growth by application of external force generated from the electric field [48]. The external forces can also be created by other means such as interaction with substrate, gas flow, etc. [49, 50]. A zigzag morphology of nanotubes may contain 2–4 sharp and alternating bends at 90° angle. A DC plasma-induced CVD may generate CNTs of such structural morphology [51]. The change of direction of electric field in the growth region induces bending in nanotubes.

6.2.2.5 Coiled Carbon Nanotubes

Coiled CNTs are formed when a pair of heptagon and pentagon arrange in a periodic fashion inside a hexagonal network of carbon [52]. Helical structures of carbon have been evidenced in the early fifties [53]. Coiled CNTs are synthesized in the year of 1994 [54]. In recent practice, coiled CNTs are synthesized by catalytic CVD technique on iron coated with indium tinoxide substrate [55]. This process produces more than 95% of helical CNTs of different diameters and pitches. Study reveals that indium and tin have a major role in the formation of coiled CNTs [56]. A study on the thermodynamic model explains the reason behind the formation of coiled structures in CNTs [57]. They suggest that interaction between the particular metal catalysts and growing nanostructures plays remarkable roles in deciding the possibility of the helical growth of CNTs. Coiled CNTs are useful for applications such as sensors, electrical inductors, nanoscale mechanical springs, electromagnetic wave absorber.

6.2.2.6 Beaded Carbon Nanotubes

Beaded CNTs are formed in different patterns, and structurally, they can be either amorphous or polycrystalline graphite. The beads can be present either with or after the formation of CNTs [58, 59]. Beaded CNTs can be occasionally formed from the interior of arc deposition. The beads are amorphous phases of carbon glass. They occur during the growth of the nanotubes since the carbon-coated CNTs are viscous liquid form and cooling leads the increment in viscosity to a great degree that beading stagnated. Bead formation in CNTs may take place during low-temperature CVD process [59]. CNTs with beads can be useful as fillers to be incorporated in composites. Incorporation of them in composites is effective to improve mechanical and electrical properties of the composites since the presence of beads prevents slippage of nanotubes [31].

6.3 Synthesis of Carbon Nanotubes

The oldest method of synthesis of CNTs is electric arc discharge, which has been used in the sixties for the production of carbon fibers as well. Later on, in 1990, this very old method has been used for the production of fullerenes and subsequently for the development of MWNT and SWNT. Other popular methods of synthesis of CNTs are laser ablation, chemical vapour deposition (CVD), etc. The laser ablation process is technically similar to that of the arc discharge method; only the difference remains in purity and quality of CNT produced. The complete synthesis routes of CNTs can be classified under three main classes such as physical, chemical, and other methods as represented in Fig. 6.4. Other methods of CNT production such as electrolysis, solar techniques, hydrothermal process, etc., will also be discussed in this chapter.

6.3.1 Physical Methods

6.3.1.1 Arc Discharge

In the arc discharge method, two highly pure graphite electrodes are used. The anode material used is either a pure graphite or metal. In case the metal anode is used, metal is mixed with graphite and kept in a hole made at the centre of the anode. The electrodes are shortly contacted, and arc is hit. The synthesis has been carried out in an inert atmosphere or an environment of reactant gas under low-pressure range (30–130 or 500 torr). The distance between the two electrodes is reduced until current flows (50–150 A). A consistent gap is maintained between the cathode and anode by

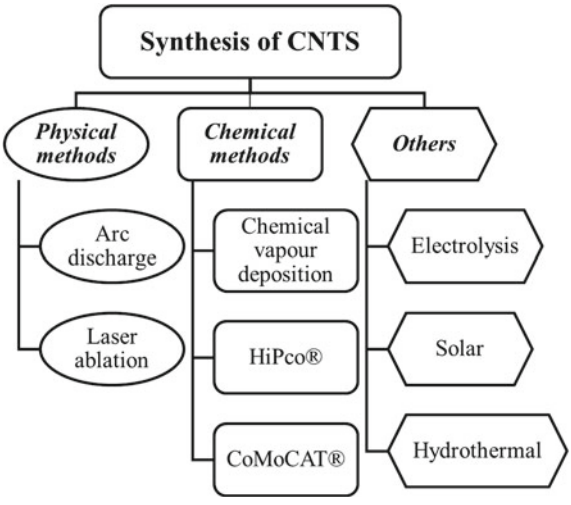

Fig. 6.4 Different routes of synthesis of CNTs

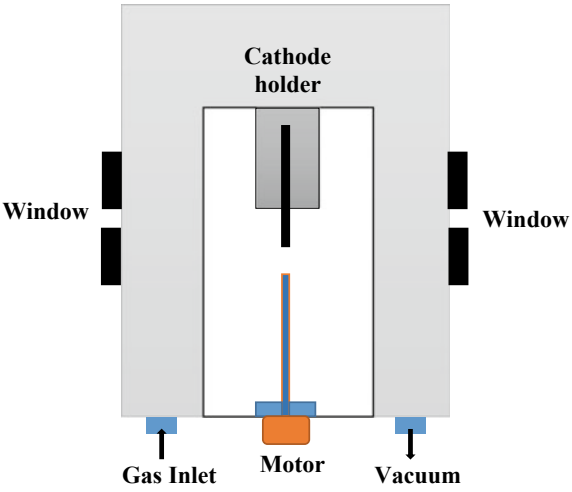

Fig. 6.5 Outline of arc discharge method

changing the anode position. A plasma is hence formed, and the stabilization of this plasma has been done by controlling distance between the cathode and anode. The reaction time varies from a few seconds to a few minutes. The arc discharge method is schematically represented in Fig. 6.5.

Different products are formed at different parts of the reactor. For examples, huge quantities and types of soot are formed on the wall of the reactor, web-like carbon morphology between the cathode and wall of the chamber, around the cathode deposit sponge collaret, at cathode end deposition of grey hard materials, etc. The product may contain amorphous and polyhedral carbons, encapsulated metallic particles, etc. [60]. The metals used for the synthesis of CNTs are Fe, Mo, Co, Y, Ni, etc., one at a time or in mixtures. In the absence of catalysts, soot and deposits are the major products in this process. Fullerene can be found in soot, whereas the MWNT and graphite carbon nanoparticles have been evidenced in the carbon deposits. In this process, nanotubes formed are of diameter in the range of 1–3 nm having an outer diameter of 2–25 nm. The tube lengths are usually of about one micron with closed tips of nanotubes. For the synthesis of SWNTs, they are devoid of any catalysts and either remain as isolated or in bundles. SWNTs are made of a diameter of about 1.1–1.4 nm with a length of a few microns.

The product quality of arc discharge method depends on several factors such as concentration and dispersion of carbon vapour in inert gas, catalyst composition, reactor temperature, presence of hydrogen and addition of promoter [61–63]. These are the major factors controlling the types of nanotubes (SWNT or MWNT), nucleation and growth mechanism of nanotubes, inner and outer diameter, length of the nanotubes. The study reveals that the use of hydrogen inside the reactor reduces the formation of carbon nanoparticles [61]. In addition, other major factors affecting the quality of nanotubes are pressure of reactant gas and type of discharge methods. Shi et al. showed that for helium gas environment at a pressure of 700 torr produces

SWNT bundles having a diameter of 20–30 nm and length of 15 μm [64]. Under the same condition only, changing the pressure to 300 torr produces a mixture of fullerene and metallofullerene indicating the influence of reactant gas pressure on the production of nanotubes [64]. Different ways of arc discharge such as intermittent or plasma rotating arc discharge methods are used for the development of nanotubes. Intermittent arc discharge produces carbon nano-onions with nanotubes [65]. The main technical part in the process of arc discharge is that it uses pulse duration for several milliseconds, which is quite long compared to the microsecond pulse duration for the pulsed arc process. The products of this process may be straight MWNT of 100–500 nm long and aggregated onion-like carbon nanoparticles. For the plasma rotating arc discharge method, the increase in rotation speed improves the yield of nanotubes as the collector comes more and more close to plasma [66].

6.3.1.2 Laser Ablation

SWNT has been synthesized by Guo et al. by utilizing the pulse laser ablation method [67]. In 1996, a successful approach has been taken by Smalley for the mass production of SWNT by the laser ablation method [68]. Nanotubes obtained by the laser ablation process are of the high purity of about 90%, and their structures are found to be better graphitized as compared to those obtained by arc discharge method. However, the major disadvantage of this method remains a small carbon deposit. Laser ablation method favours the growth of SWNTs, and MWNTs can only be formed under special reaction conditions. In a typical synthesis method, a laser beam of 532 nm has been focused on a composite target made of metal and graphite. The target has been placed in a high-temperature furnace at 1200 °C. The laser beam scans across the surface of the target material to control the smooth and uniform face of vaporization. The soot produced has been swept by argon flow from the high-temperature zone of the furnace to the copper collector. The target material has been formed by uniform mixing of metal and graphite in the form of a rod in three steps: first, a paste is formed by mixing metal, graphite, and carbon cement at room temperature and subsequently introduced in the mould; second, the mould has been kept in a hydraulic press and baked at 130 °C for 5 h at a constant pressure. In the final step, the curing of rod has been performed by heating at 810 °C for 8 h under argon atmosphere following by heating at 1200 °C for another 8 h. The metal used in the process is Co, Ni, Ni/Pt, Co/Cu, etc. The synthesis of nanotubes by laser ablation method has been schematically represented in Fig. 6.6.

The nanotubes formed by laser ablation method are accompanied by amorphous carbon, fullerene, catalyst particles, and graphite. Other impurities found are silicon and hydrocarbons, which may be from unknown sources [67]. The product quality of this process depends on a number of parameters such as ratio and types of metal catalyst particles [69, 70], ambient gas type and pressure [71, 72], laser-related parameters [73], and furnace temperature [74]. The properties of the nanotubes much dependent on laser parameters such as peak power, continuous wave (cw) versus pulse, oscillation wavelength, rate of repetition. Other contributing factors are composition of

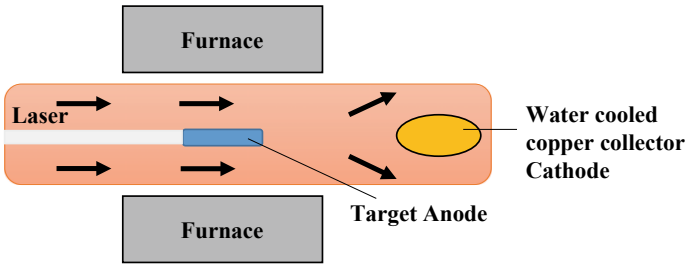

Fig. 6.6 Schematic representation of laser ablation method for synthesis of CNT

target material, pressure inside the chamber and its chemical composition, substrate types, distance between the target and substrate, etc. To date, the relation between excitation wavelength and growth mechanism of nanotubes is not clear. Possibilities are UV laser creates new nanoparticle materials suggesting a new growth mechanism. The UV laser is much better than infrared laser, which is more effective in photothermal ablation. Lebel et al. reported the synthesis of SWNTs from the UV laser ablation method. The target material used is graphite doped with Co/Ni metal catalyst and examined for the reinforcing ability in polyurethane [75].

Both arc discharge and laser ablation processes produce good quality of nanotubes; however, due to the several drawbacks as mentioned below, the industrial production of nanotubes by these processes is limited. These two processes are somehow energy-extensive methods hence uneconomical for large-scale production of nanotubes. The nanotubes prepared by those methods are impure and require extensive purification steps. These additional purification steps are difficult as well as expensive in view of large-scale production. Hence, other synthesis methods are developed for large production of high-quality pure carbon nanotubes.

6.3.2 Chemical Methods

6.3.2.1 Chemical Vapour Deposition

Chemical vapour deposition (CVD) method of synthesis of CNTs is based on the catalyst-induced decomposition of carbon monoxide or hydrocarbons with the help of supported transition metals as catalysts. The chemical reaction proceeds in a flow furnace kept at atmospheric pressure. There are mainly two types of furnace—one is vertical, and the other is horizontal. The horizontal furnace is the most popular one. In horizontal furnace configuration, the catalyst particles are kept in a quartz or ceramic boat placed inside a quartz tube. The reaction mixture is composed of a hydrocarbon source and inert gas, which are then passed over the catalyst to commence the reaction. The temperature of the furnace is kept from 500 to 1100 °C. After the desired reaction time, the furnace is cooled down to ambient temperature.

The vertical configuration is employed for the synthesis of large quantities of carbon fibers and nanotubes. Here, the catalyst and source of carbon are together introduced at the top side of the furnace and the products are formed during flight, which are subsequently collected at the bottom of the furnace. Fluidized bed reactor is another popular form, which is typically a modified version of vertical furnace configuration. Figure 6.7 shows all three types of CVD set-up in a simple diagram. The supported catalysts are placed in the furnace centre, and carbon feedstock in gaseous form is introduced via upward flow. In this process, supported catalyst experiences much longer time residence inside the furnace than the vertical furnace types [76]. In a generalized way, nanotubes grow in a CVD process by dissociation of hydrocarbons in the presence of transition metal catalysts. The carbon gas precipitated from the catalyst particles leads to the progressive formation of tubular carbon solids in sp^2 structure [77].

Chemical vapour deposition technique is of different types, such as catalytic CVD (CCVD) can be thermal or plasma-enhanced (PE) techniques, which are a common standardized method of CNTs production in recent days [78]. Other common types of CVD techniques are water-aided CVD [79, 80], oxygen-assisted CVD [81], radiofrequency CVD [82], hot-filament CVD [83], and microwave plasma CVD [84, 85].

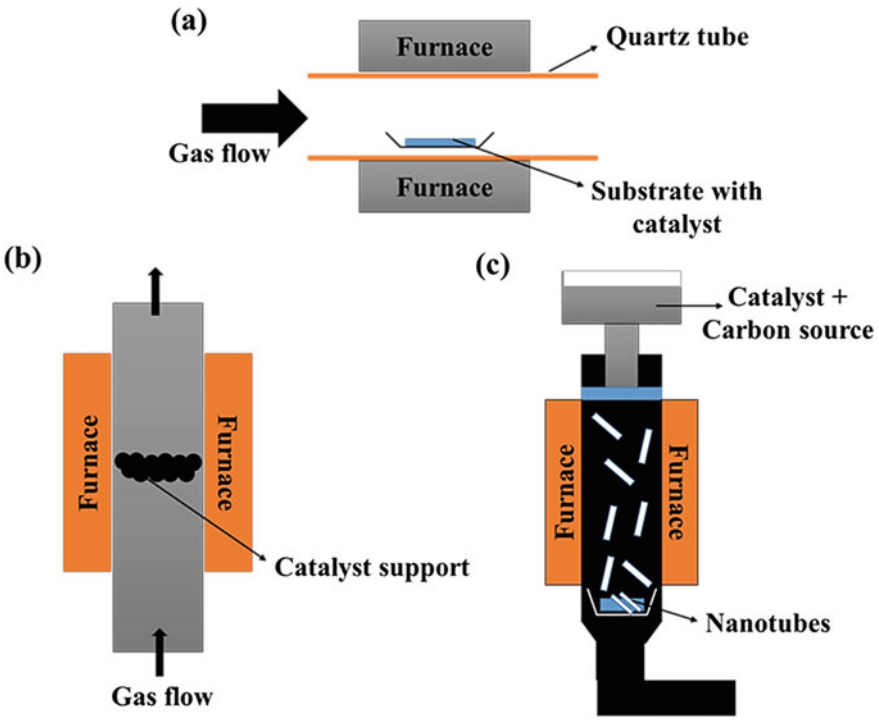

Fig. 6.7 Schematic representation of simplified CVD set-up, **a** horizontal furnace, **b** fluidized bed reactor, and **c** vertical furnace

Catalysts play a major role leading to the decomposition of the carbon sources either by plasma treatment (PECVD) or by heat effect (thermal CVD). PECVD can again be operated at different modes such as radio, direct current, diffusion, microwave named as RF-PECVD, DC-PECVD, D-PECVD, MW-PECVD, respectively. The most common catalysts are transition metals, i.e. Fe, Co, and Ni [86]. In some cases, these traditional catalysts are mixed with other metals such as Au [87]. The examples of carbon sources are various hydrocarbons and their mixtures, ethanol, etc. [88–90]. For gaseous source material, the growth of CNTs is dependent on the reactivity and gas-phase concentration of the intermediates generated by decompositions of hydrocarbons. The common substrates used for the synthesis of CNTs by CVD method are Ni, SiO_2, Cu, Si, stainless steel, graphite, tungsten foil, etc. [91, 92]. A special substrate of mesoporous silica can also be used, where it may also play the role of a template material controlling the growth of nanotubes [93].

The quality of nanotubes formed in the CVD depends on a number of parameters such as operating temperature and pressure, hydrocarbon types, volume and its concentration, metal catalyst types, nature and its pre-treatment process, nature of support materials, and the overall reaction time [94]. CCVD is considered as the most successful method of CNT production, and the quality of the CNT is much better compared to the laser ablation method. The development of pure CNT with the provisions of large-scale production is the main advantage of this technique.

6.3.2.2 High-Pressure Carbon Monoxide Process (HiPco®)

This method is developed for the synthesis of CNTs in 1999 [95]. This method stands different than others in the sense that here catalyst has been introduced in gaseous form. Both catalyst and hydrocarbon in gaseous form feed into the reactor or furnace. This method is particularly suitable for large-scale synthesis of CNTs since the synthesized nanotubes will be free of catalytic support and the reaction may proceed continuously. In general, CO is used as a source of hydrocarbon gas, which reacts with $Fe(CO)_5$ to generate SWNT. This process is popularly known as HiPco® process. SWNTs are also produced with a slightly modified HiPco® process where a mixture of benzene, ferrocene, and $Fe(C_5H_5)_2$ undergoes reaction in a flow of hydrogen to form SWNT [96]. In these two processes, catalyst nanoparticles are generated by thermal decomposition of organometallic compounds, e.g. ferrocene and $Fe(CO)_5$.

6.3.2.3 CoMoCAT® Process

In another method known as CoMoCAT process, cobalt and molybdenum are used as a catalyst with CO gas for the synthesis of CNTs [97]. In this method, SWNTs are grown by the disproportionation reaction of CO forming C and CO_2 in the presence of this special catalyst at 700–950 °C under a total pressure of 1–10 atm in the flow of pure CO. This process is successful to grow a considerable amount of SWNT in a few

hours with a selectivity ratio higher than 80%. About 0.25 g of SWNTs are formed per gram of catalyst. The specially designed catalyst combination is effective to induce synergism in catalytic performance. The nanotubes formed by HiPco process produce a number of bands indicating more variation in the diameter of nanotubes compared to the CoMoCAT process. Again, the diameter distribution by the HiPco process remains significantly greater compared to that in the CoMoCAT process. Hence, this process has a great potential to be scaled up for the large-scale industrial production of SWNTs.

6.3.3 Others

6.3.3.1 Electrolysis

One of the unorthodox methods of CNT production is by electrolysis developed by Hsu et al. in the year of 1995 [98]. In this method, an alkali or alkaline earth metal is electrodeposited on a graphite cathode followed by nanotube production by the interaction of the electrodeposited metal on the cathode. The temperature for the synthesis of the nanotubes varies from the electrolyte to electrolyte; for example, for NaCl and LiCl as electrolytes, the temperature is kept just above the melting point of the salt. Once the electrolysis is completed, the carbonaceous materials are collected by the dissolution of ionic salts in water followed by filtration. During the electrolysis, cathode erodes. In this method, the main impurities are carbon nanoparticles of different structures, amorphous carbon, carbon-encapsulated metals, carbon filaments, etc. Electrolysis produces mainly MWNTs; however, SWNTs are also grown [99]. In this study, nanotubes are prepared by electrolysis using NaCl at 810 °C under argon atmosphere by electrolytic conversion of graphite to nanotubes. SWNTs obtained in this method are comparable to that synthesized from other standard methods, and the diameter remains in the range of 1.3–1.6 nm.

6.3.3.2 Solar

Another method of nanotube production is using solar energy. This process is utilized around 1996 mainly for the production of fullerenes. Laplaze et al. have demonstrated the method of production of carbon nanotubes using solar techniques [100]. In this method, carbon and catalyst, in mixed form are vaporized by incident solar energy. A high-flow vacuum pump is used to maintain the inside pressure. Argon or helium is used as the buffer gas to prevent the condensation of the mixed vapours by swiping its interior surface. The solar energy is focused on the target material with the help of a parabolic mirror placed above the chamber. The vaporization temperature is in the range of 2627–2727 °C. The vaporized mixture of carbon and catalyst along with the buffer gas is then aimed to pass between the target and the graphite tube at the backside of the reactor. SWNTs are reported to be produced by solar method in

grams using 50 kW solar reactor [101]. The experimental set-up is placed in a solar furnace of 1 MW capacity. The effects of various parameters such as length of the target, location of sample collector, buffer gas have been investigated with respect to the quality of the nanotubes produced.

6.3.3.3 Hydrothermal

Hydrothermal or sonochemical process is another alternative synthesis methodology used for the development of various carbon-based nanoarchitectures such as nanorods, nanobelts, nanowires, nano-onions, MWNTs. The main advantages of this process over others are, the starting materials are stable at ambient temperatures and are abundant, and it is a low-temperature economical process; the temperature range is about 150–180 °C, and there is no need of hydrocarbons or carrier gas, etc. MWNTs are successfully prepared by the hydrothermal method from a mixture of polyethylene and water in the presence of Ni as catalyst. The temperature and pressure are kept in the range of 700–800 °C and 60–100 MPa [102]. MWNTs of closed and open tube ends of more than 100 carbons are produced by this method. One of the specific features of MWNTs produced from the hydrothermal method remains that the nanotubes are of small wall thickness and a large core diameter of about 20–800 nm. In another study, graphitic nanotubes are prepared by the use of ethylene glycol with Ni catalyst under the temperature and pressure condition of 730–800 °C and 60–100 MPa [103]. TEM analysis of the nanotubes reveals the fact that the nanotubes are long and have wide internal channels, and the catalyst particles are located at the tip positions. The wall thickness of nanotubes prepared by this method remains in the range of 7–25 nm with an outer diameter of 50–150 nm. This method is also suitable to produce nanotubes with a thin wall having the internal diameter in the range of 10–1000 nm.

The growth mechanisms of CNTs are still not known exactly. New synthesis methods are focused to be developed with the aim of high yield, purity, and fewer defects at low cost. Among the methods commonly employed for the synthesis of nanotubes, CVD is found to be best for large-scale production of MWNTs. Variants of CVD processes such as CoMoCAT® and HiPco® may be scaled up for large-scale industrial production of CNTs. Production of SWNTs via CVD method still needs attention since the yield is only in grams and they are mixed with helical CNTs.

6.4 Growth Mechanism of Carbon Nanotubes

The growth mechanisms of CNTs are still not concrete. Based on reaction parameters and post-analysis of products, several groups have proposed different mechanisms. MWNT grows without the use of any catalyst particles in arc discharge and laser ablation methods, whereas CVD method requires the use of metal particles as catalysts. However, to grow SWNTs, the need for catalysts is essential. Hence, the

growth mechanism of CNTs varies from methodology to methodology depending on the number of parameters. The growth of CNTs synthesized by CVD techniques depends on catalyst particle size and concentration, growth time and temperature, pressure, gas flow rate, etc. The common mechanisms proposed for the growth of CNT are *vapour-solid-solid (VSS)* and *vapour-liquid-solid (VLS)* mechanisms.

6.4.1 Vapour-Solid-Solid (VSS) Mechanism

In this mechanism, the growth of CNTs can be explained by four steps [104]. At the beginning, nanoparticles of metal catalysts are formed on the substrate, which are deformed either by laser ablation or by heating to a thin metallic film. In the next step, decomposition of hydrocarbon gas proceeds over the catalyst surface leading to the release of hydrogen and carbon. In the third step, carbon diffuses through the metal particles and precipitated. Finally, in the last step, overcoating and deactivation of metal catalysts lead to the termination of nanotube growth. The growth of CNT is commonly described by two mechanisms involving the metal particles called as tip-growth and base-growth mechanisms. In the tip-growth mechanism, metal particles detach and move towards the head of a nanotube. Continuous growth process reveals that the nanotubes grow at the support side having the metal particles lifted at the tip side of the tubes. The movement of catalyst particles towards upside is due to the diffusion and osmotic pressure leading to the continuous deposition of carbon below the catalyst particles. In this case, the interaction between the catalyst and substrate remains weak, and hence, hydrocarbon decomposition takes place on the top of the metal particle surface followed by diffusion of carbons through the metal. This leads to precipitation of CNTs across the bottom of the metal particles and pushes off the entire metal particles from the substrate. This process continues as long as the metal surface is available for the decomposition of hydrocarbon and the concentration gradient is present with progressive growth of length of nanotubes. Once the metal particle is completely covered with carbon, the catalytic activity is over and termination takes place. The complete growth process by tip-growth mechanism is presented in Fig. 6.8.

Another common mechanism of nanotube formation is by the base-growth mechanism. In this case, the interaction between the substrate and metal particles is strong. At the very beginning, decomposition and diffusion of carbon follow the same path as that of the tip-growth mechanism. However, the strong interaction between the catalyst and substrate prevents the CNT precipitation to push successfully the catalyst particles towards upwards, and hence, the growth of nanotubes begins from the apex of the metal since there exists least interaction with the substrate and are farthest to the substrate side. Carbon crystallizes in the form of a hemispherical dome and extends further as a seamless cylinder of graphite. Subsequent decomposition of carbon takes place at the periphery of the metal, and carbon diffuses upward. In this mechanism since growth of the nanotubes proceeds from root of the catalyst particles hence, named as base-growth mechanism.

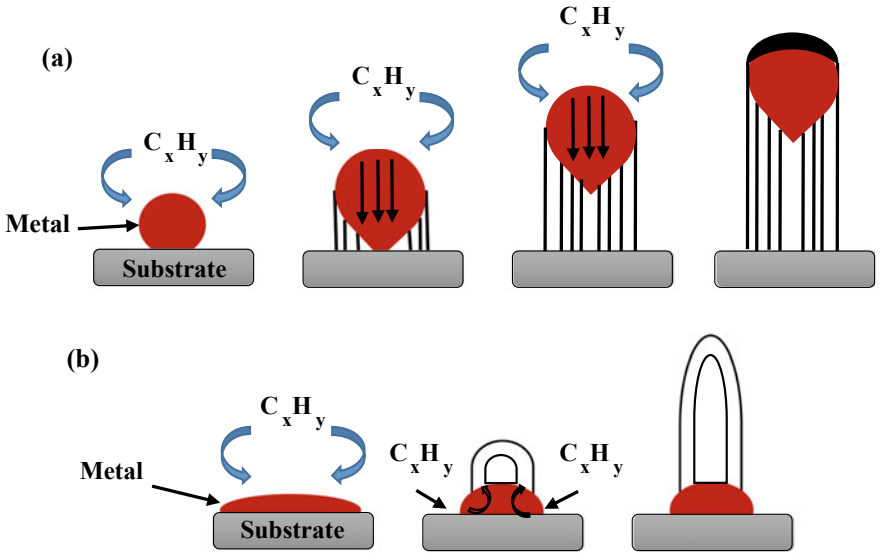

Fig. 6.8 Growth mechanism of CNT, **a** tip growth and **b** base growth

6.4.2 Vapour-Liquid-Solid (VLS) Mechanism

This mechanism consists of three stages, e.g. nucleation, precipitation and deposition. In the arc discharge method, when metal particles get evaporated with carbon, form carbon-metal alloys on the cathode side. At the start, the alloy remains in liquid state due to the high temperature at the cathode surface and reduction of melting point takes place during alloy formation. Since, the soot produced in this case is in a carbon-rich atmosphere, the alloy in liquid phase contains higher amount of carbon over its solubility limit as that in solid state. Thereafter, as the temperature of the cathode falls the alloy begins to segregate. This mechanism is acceptable to a great level; however, the state of alloy in liquid form at the process temperature of about 600–900 °C is still debatable. Again, one important point to be considered in this respect is that the decomposition of hydrocarbon over the catalyst surface is a highly exothermic reaction, which may add some value to the statement of liquid state of metals. This mechanism has been supported by scientists for the growth of SWNTs [105]. Figure 6.9 displays the growth mechanism of SWNTs at different temperatures. However, for MWNTs and large metal particles, this point is still to be explained. As the bigger particles are expected to be preferably in solid phase, a different mechanism is to be followed for MWNT and SWNT. As a concluding remark, we come to our initial statement; the growth mechanism is still a matter of debate, and the different outlooks are present based on the reaction and process parameters.

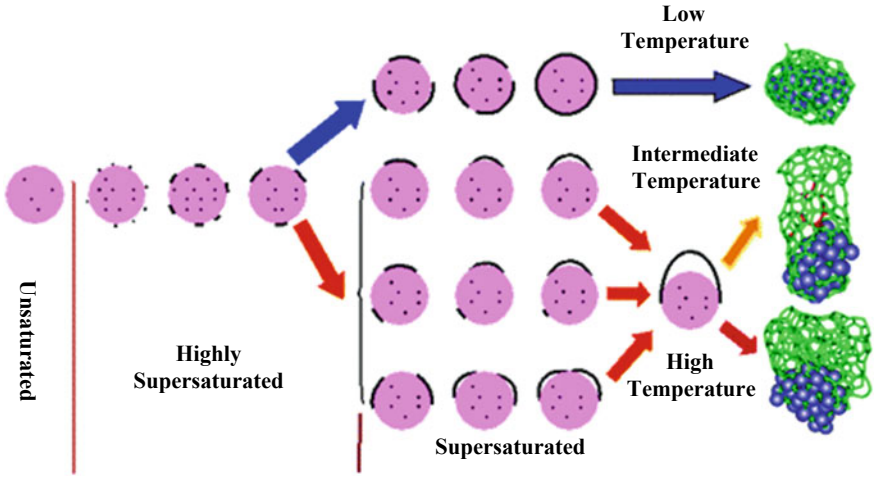

Fig. 6.9 VLS mechanism showing growth of SWNTs at different temperatures. Redrawn and reprinted with permission from [105]

6.5 Purification of Carbon Nanotubes

Depending on the method of preparation of CNTs, different approaches are taken to purify the synthesized CNTs. In addition to the large-scale synthesis hurdles, the purifications of CNTs are also a challenging aspect. In general, the purification procedures of CNTs can be broadly classified into three classes, namely gas phase, liquid phase, and intercalation methods. In the gas-phase purification process of CNTs, it has been evidenced that the process of oxidation remains easier for defective nanotubes compared to relatively perfect ones. NASA Glenn Research centre, in 2002, has introduced a new gas-phase purification process using high-temperature oxidation and repeated the treatment with nitric and hydrochloric acids for SWNTs [106]. This process is found to be suitable due to the improvement in nanotube stability. The liquid-phase purification methods mainly include filtration, dissolution, microfiltrations, centrifugal, and chromatographic method of separations. For liquid-phase purification, the CNTs undergo hydrogen peroxide-based liquid-phase oxidation to remove the amorphous carbons. Intercalation of CNTs is another method to obtain clean CNTs using $CuCl_2$ to oxidize the nanoparticles. In this technique, in the first stage, cathode is subjected to immersion in molten form of copper and potassium chloride mixture for some days under temperature. The excess chlorides are then removed by the process of ion exchange. The intercalated copper and potassium chloride metals are then heated in a reactive environment of hydrogen or helium. Afterward, the oxidation of the intercalated compound has been performed in flowing air with simultaneous heat treatment. This easy method, however, suffers from drawbacks of loss of CNTs at the oxidation stage with chances of contamination from intercalates.

The main steps followed for the purifications of CNTs are removal of big graphite particles and agglomerations by filtration, dissolution of the CNTs in proper solvents to remove the catalyst particles, removal of amorphous carbon parts from CNTs, microfiltration and chromatography for size separation [107]. SWNTs can be purified by ultrasound assistant microfiltrations and size exclusion chromatography. The catalyst particles and amorphous carbons are successfully removed producing clean nanotubes [82, 84]. Again, the above-mentioned common impurities from SWNTs are also removed by treating with nitric and hydrofluoric acids as well [83, 108]. Based on the diameters of SWNTs, density gradient ultracentrifugation has been used [109]. Size exclusion chromatography has also been utilized for the purifications of SWNTs in a recent study [110]. A combined method of ion-exchange chromatography and DNA dispersion has been used for the purification of SWNT based on the concept of chirality. Common methods of fluorination and bromination have also been utilized to purify MWNTs and SWNTs by suspending CNTs in suitable organic solvents [111, 112].

The main impurities present in CNTs are graphite, fullerenes, amorphous carbon and metal catalyst particles. The common industrial techniques used for the purification of nanotubes are oxidations, acid reflux, etc. Figure 6.10 shows the different routes of purification of CNTs. However, major difficulties in these techniques are its adverse effect on the structure of the nanotubes, insolubility of nanotubes also limiting the provisions of liquid chromatography. Removal of impurities from CNTs affects its surface area, porosity, pore-volume, introduction of additional functional groups over the CNT surface, removal of blockage at the entrance of the pore by selective decomposition of functional groups, etc. All of these have a significant effect on the ultimate properties of the nanotubes.

Oxidation of nanotubes is done with the aim to remove carbon-containing impurities [113]. However, the major drawback remains that the process of oxidation oxidizes the nanotubes as well with impurities, likely to make some damage in its structure. However, the fact is, the damage on the nanotubes is quite less as compared to impurities since the impurities have a more open structures with more defects to attack. Again, another benefit of oxidizing the impurities is that catalyst particles help the process since they are attached to these impurities. The purification of nanotubes by oxidation depends on factors like oxidizing agent, temperature, oxidation time, and metal content. Metallic catalyst particles are removed from CNTs by acid

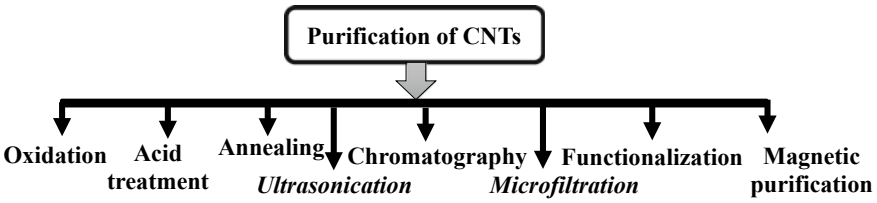

Fig. 6.10 Purification of CNTs

treatment. At first, the metal surface has been exposed by oxidative treatment or sonication, which is subsequently introduced to acidic treatment and solvation. CNTs at this point remain suspended. The best part of acidic purification by nitric acid is that the acid will only affect the metal particles and the nanotubes remain intact [114]. The mild acidic treatment has also similar utility as nitric acid reflux; however, the metal particles are needed to be exposed completely to the acids to solvate [115]. Annealing of nanotubes is carried out at high temperatures (600–1600 °C) to consume the defect and rearrange the nanotubes [116]. High temperature also helps in pyrolyse short fullerenes and graphitic carbonaceous materials. During heating under vacuum, the metal particles are melted and can also be removed easily from the nanotube as observed by Kajiura et al. [117]. Ultrasonication is one more common technique used for purification of nanotubes where particle separation is due to ultrasonic vibration. The agglomerated particles are vibrated and dispersed. The separation of the particles is very much dependant on the type of surfactant, solvent and reagents. The stability of dispersed nanotubes is affected by the nature of solvent; for e.g., the nanotubes are found to be more stable in poor solvents, when they are still attached to the metal particles of the catalyst. The magnetic impurities present in CNTs can be easily removed by using a permanent magnet. In this method, the catalytic magnetic particles are effectively removed from graphitic shells [118]. The CNTs in suspended form are mixed with ZrO_2, $CaCO_3$, etc., in an ultrasonic bath. The magnetic particles are trapped by a permanent magnet later. This process of magnetic separation is useful since no large equipment is needed and laboratory size quantity of CNTs free of magnetic impurities can be prepared very easily by this process. The particle-based impurities such as catalyst particles, carbon nanoparticles, fullerenes can be effectively removed from CNTs by microfiltration [114]. Fullerenes are removed by microfiltration approach by treating with CS_2 solution. The filter traps CS_2 insoluble. The fullerenes solvated in CS_2 is only able to pass through the filter [115]. Functionalization is another approach to prepare clean CNTs. Functionalization makes CNTs soluble by attachment of suitable chemical entities to the nanotubes. This enables to separate the CNTs easily from insoluble impurities such as metallic catalyst particles [119]. Chemistry of functionalization of CNTs has been summarized in Fig. 6.11. CNTs can also be cleaned by other functionalization where the structure of nanotubes is kept intact and they remain soluble for preferable chromatographic separation [116]. After the purification step is over, the functional groups are usually removed by heat treatment or annealing. All the purification processes employed for CNTs lead to a little bit of structural changes in CNTs. This changes the properties of CNTs as well. Hence, during purification of nanotubes, the motto should be to remove the carbonaceous impurities and metals with no or minimal change in its tube structure. Extra care is to be taken when choosing the time, temperature, and chemicals. Again, economical and large-scale techniques are of utmost importance for successful large-scale synthesis of pure CNTs.

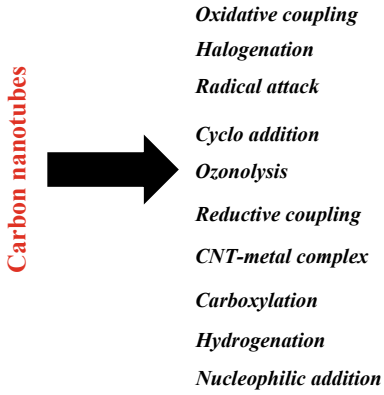

Fig. 6.11 Chemistry of functionalization of CNTs. Drawn based on the concept taken from [120]

6.6 Properties of Carbon Nanotubes

In recent years, CNTs have progressively attracted the attention of scientific community due to the excellent combination of electrical, mechanical, thermal, etc., properties. The alteration in tube structure enables tailoring of the nanotube properties making it a material of choice in different application domains.

6.6.1 Electrical

The electrical properties of CNTs are dependent on its structure to a great extent. Nanotubes with armchair configuration behave like metal, and when a voltage is applied at the end of these nanotubes, current flows. The other two configurations, namely zigzag and chiral, behave as semiconductors. In these two forms, the nanotubes conduct electrical current when extra energy is supplied to generate free electrons from carbon. Semiconducting CNTs are of importance in electrical devices, transistors and integrated circuit, etc. Again, the electrical resistance of CNTs can be changed remarkably when attached to other molecules. These specific electrical properties of CNTs are useful for their applications as sensors to detect carbon monoxide. Hence, the structural arrangements of carbons in CNTs open provisions to be explored as interconnects and functional materials to enhance conductivity in polymeric composites. Researchers are also aiming to fabricate electrically conducting nanowires entirely made of CNTs. However, challenges remain to overcome the resistivity at the connection of two nanotubes, where the conductivity is reduced by orders of magnitude compared to the individual one.

The electrical conductivity of nanotubes having current carrying capacity is a thousand times better than copper as reported [121]. An isolated nanotube exhibits electrical conductivity of 2×10^7 S m^{-1} and ampacity of 10^{13} A m^{-2} [122, 123]. Based on the method of producing, CNT materials can be of eight different types. They

are broadly classified into three main categories—the first-class deals with vertically aligned CNTs made of CVD technique also named as CNT forest. They may be densified in the form of pillars, spun into fibers, drawn in form of a mat. The second category fabricates CNTs from the solution phase. They can be made in the form of a mat by filtration of the CNT dispersed liquid, named as buckypaper or can be fabricated in the form of single fiber as well. Porous CNT foams can also be produced from aqueous gel. The last category is obtained by direct spinning of CNT aerogels producing direct spun fibers and mats depending on the fabrication procedure [124]. Below in Fig. 6.12, variation of electrical conductivity of different categories of CNTs has been shown with respect to density.

Other than the method of fabrication, the transfer of phonon or electrical conductance in CNTs also depends on the length of the nanotubes [125]. As per the theory of percolation, electron transfer is achieved with a lesser number of nanotubes when

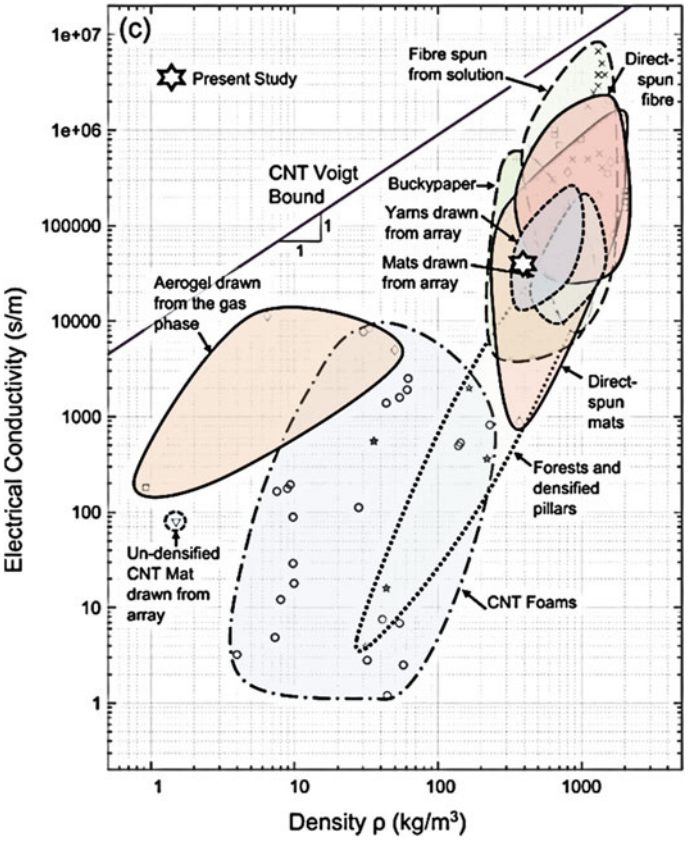

Fig. 6.12 Electrical conductivity as a function of density of different CNT materials. Reprinted with permission from [124]

long CNTs are used. The percolation threshold and length of the nanotubes are governed by the equation $N_c = 5.71/L_s^2$, where N_c and L_s represent the percolation threshold and length of nanotube [126–128]. Studies report that much better electrical conductivity has been achieved for transparent films made of long CNTs [129, 130]. Long CNTs are also beneficial to improve the properties of CNT/polymer composites due to fewer nanotube junctions [131, 132]. CNTs are of high aspect ratio, and hence, a low loading of nanotubes will be sufficient to achieve desired conductivity. The high aspect ratio of nanotubes makes the electrical conductivity of these materials comparable to that of conventional additives such as stainless steel fiber, carbon black, and carbon fibers, etc.

6.6.2 Mechanical

CNTs are stiffest and stronger fibers ever produced. The Young's modulus of CNTs can be as high as five times more than steel with a tensile strength of 50 times better than steel. These unique properties of CNTs combined with low density make them a potential candidate for structural applications. Common practice is being incorporation of these materials to the polymer matrix to fabricate high strength composites for structural and electrical applications. In CNTs, each carbon in a graphite sheet is connected with a strong chemical bond to three neighbouring carbon atoms. Hence, CNTs are of strong basal plane elastic modulus and is a fiber of high strength. The elastic modulus of SWNTs remains higher than steel making them a highly resistive material. Pressing at the tube ends although it leads to bending of the tubes; however, the nanotubes soon return back to its original state as soon as the force is removed. This particular character of CNTs opens up the possibilities to be used as tips of high-resolution scanning probe microscopy.

The mechanical properties of nanotubes can be explained from the general properties of a graphene sheet. The interaction is weak van der Waals force acting among the sheets of the graphene. The interlayer distance of a typical sheet of graphene is 0.335 nm [133]. The interlayer elastic modulus of MWNTs is comparable to that of graphite of 1.04 TPa having a shear strength of 0.48 MPa, which is of the same order as that for graphite [134]. Lei et al. developed a mathematical model to calculate the mechanical properties of SWNTs, where carbon–carbon bonds are considered as Euler beams [135]. Figure 6.13 displays the effect of radius in nm on Young's modulus of SWNTs. Model predicts that the Young modulus of SWNT gradually lowers with tube radius. The modulus of armchair configuration attains a bit higher compared to zigzag one. As the radius increases further, the two horizontal lines try to become constant and approach the value of 1.0424 TPa, i.e. Young's modulus of the sheet of graphene.

Overney et al. obtained Young's modulus of SWNTs of about 1.5 TPa approximately equal to graphite [136]. Soon after, other works on the calculation of Young's modulus of nanotubes appear close to 1 TPa irrespective of tube type and diameter [137]. These results are fitted in MD simulations by Yakobson et al. taking thickness

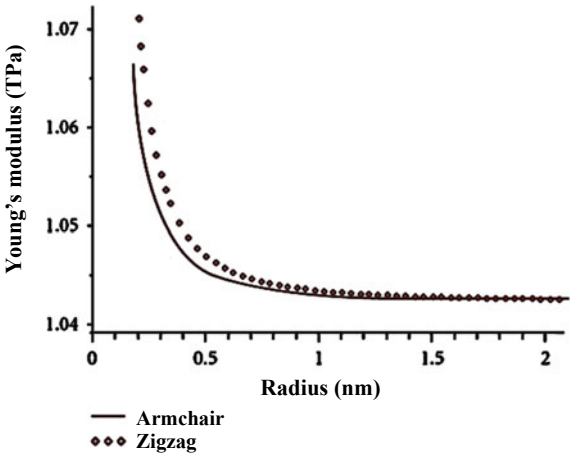

Fig. 6.13 Variation in Young's modulus with nanotube radius in nm as predicted by mathematical model. Redrawn and reprinted with permission from [135]

and modulus as fitting parameters and obtained a thickness of 0.066 nm with Young's modulus of 5.5 TPa [33]. Yokobson et al. proposed the dislocation theory explaining the mechanical relaxation of nanotubes under tensile load using molecular dynamics [138]. For tensile strain greater than 5%, dislocation consisting of pentagon and heptagon (5-7) dipole via bond rotation is observed to be the most favourable relaxation in CNTs under tensile strain. The dislocation of type 5-7-7-5 separates in two pairs of 5-7 resulting in ductile transformation under stress. Again, the dislocation of the type 5-7-7-5 may grow a crack leading to brittle fracture as well. The ductile transformation leads to the formation of tubes of smaller diameter and new chiral symmetry. The determination of mechanical properties of individual SWNTs has not been explored yet, and mechanics related to CNT is to be further investigated in detail [139, 140] In addition, the investigation on functionalization of nanotubes and associated interface mechanics at the nanoscale are still very challenging [141, 142].

6.6.3 Thermal

CNTs are good thermal conductors along the tube however act as an insulator lateral to the tube axis. The conductivity measurement of SWNT at room temperature shows a value of 3500 W m^{-1} K^{-1} compared to thermally conductive cooper of 385 W m^{-1} K^{-1} indicating its huge potential [143]. Study of thermal conductivity of CNTs confirms that the value goes to about 3000 W/mK for MWNTs [144]. The direct measurement of thermal conductivity of single nanotubes is difficult due to the technological constraints of testing in nanoscale [145]. This is the reason why thermal conductivity measurements of CNTs are mostly based on simulations and indirect experimental measurement procedures [146, 147]. The thermal transport in CNT is assumed to take place by phonon conduction process. The phonon transport

in CNTs is governed by different parameters, e.g. boundary for surface scattering, mean free path length for phonons, number of phonon active modes, etc. [148, 149]. The thermal conductivity of nanotubes depends on a number of parameters such as atomic arrangements to form the tubes, diameter, and length, structural defects and morphology, and the presence of impurities [150, 151]. Again, the presence of crystallographic defects strongly affects the thermal properties of the nanotubes. Defects increase the scattering of phonons increasing the rate of phonon relaxation; hence, a reduction in thermal conductivity is expected. CNTs can be superconductive below 20 K due to strong C–C bonds of graphene. This strong C–C bond provides exceptionally high strength and stiffness in nanotubes. The aggregation tendency of SWNT compels to measure the conductivity of single nanotubes in the form of mats [152]. Hone et al. determined the thermal conductivity of SWNT at room temperature for highly pure mats composed of nanotubes bundles. The thermal conductivities, in this case, vary in the range from 1750 to 5800 W/mK [153]. However, it is observed that the contact resistance between the nanotubes lowers the thermal conductivity of SWNT by two orders of magnitude as compared to that measured for densely packed mat of SWNTs [154]. The presence of junctions in nanotubes affects the thermal conductivity to a great extent due to the increase in thermal resistance locally [155]. This effect, in particular, reduces the thermal conductivity of junction CNTs since lattice defects are present in the form of non-hexagonal rings of carbons at the junction of the nanotubes. Results reveal that the thermal conductivity of *X*-junction nanotubes decreases by 20–80% compared to that of straight ones [156]. The effect of tube length on thermal conductivity of CNTs is shown in Fig. 6.14. The plots are obtained by taking the model length of (3,3) CNTs at 200 K. The high thermal conductivity of CNTs makes them a material of choice for sensing, electronic and actuating devices. The incorporation of nanotubes is expected to improve the thermo-mechanical properties of the composites when introduced as a functional filler in the polymer matrix.

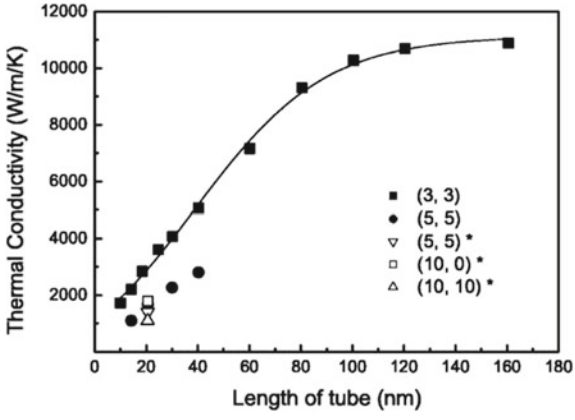

Fig. 6.14 Thermal conductivity as a function of tube length. Reprinted with permission from [156]; data used in this figure was taken from [157]

6.7 Characteristics of Carbon Nanotubes

Below we are mentioning some structural characteristic of MWNTs of interest

- Branching, if any
- Number of walls or tubes
- Concentric cylinders
- Open or capped nanotube ends
- Width or diameter of inner walls
- Ring size and connectivity
- Morphology of tubes, i.e. straight, bent, or buckled
- Molecular weight
- Catalyst particle size
- Structural defects present.

In addition to the above-mentioned structural parameters of CNTs, some important characterization of CNTs which are of general interest is as follows. These characterizations of CNTs are in practice as can be evidenced from the informal survey of vendor Webpage.

- Colour
- Purity
- Catalyst types and content
- Density
- Ash content
- % of metal oxide
- Amorphous carbon content
- Metallic impurities
- Diameter and length
- Surface area
- Raman D/G ratio indicating defects.

6.8 Application of Carbon Nanotubes

CNTs are one of the most rapid-growing nanometric materials of the modern age. The structural arrangement and hence the unique properties of CNTs make them suitable for a number of applications. Many studies are focused on the diverse application of CNTs starting from material science, biomedical, electronic, energy storage, and even CNTs as fillers as well [158]. CNTs are also useful for its high conductivity, adsorption properties, which makes them useful for applications like supercapacitors, fuel cells, energy devices, high strength composites, etc. [159–166]. CNTs because of its adsorption properties are explored in waste water treatment [167]. Below we have included a brief overview of various fields of applications of CNTs with examples

(Fig. 6.15). Instead of all these attractive combinations of properties, the use of CNTs is somewhat restricted due to the high cost and non-renewable nature. Large-scale production of pure CNTs is a point of consideration to the researcher of this field. Efforts are taken to overcome associated challenges of CNTs and to synthesize these sensational nanomaterials at low costs.

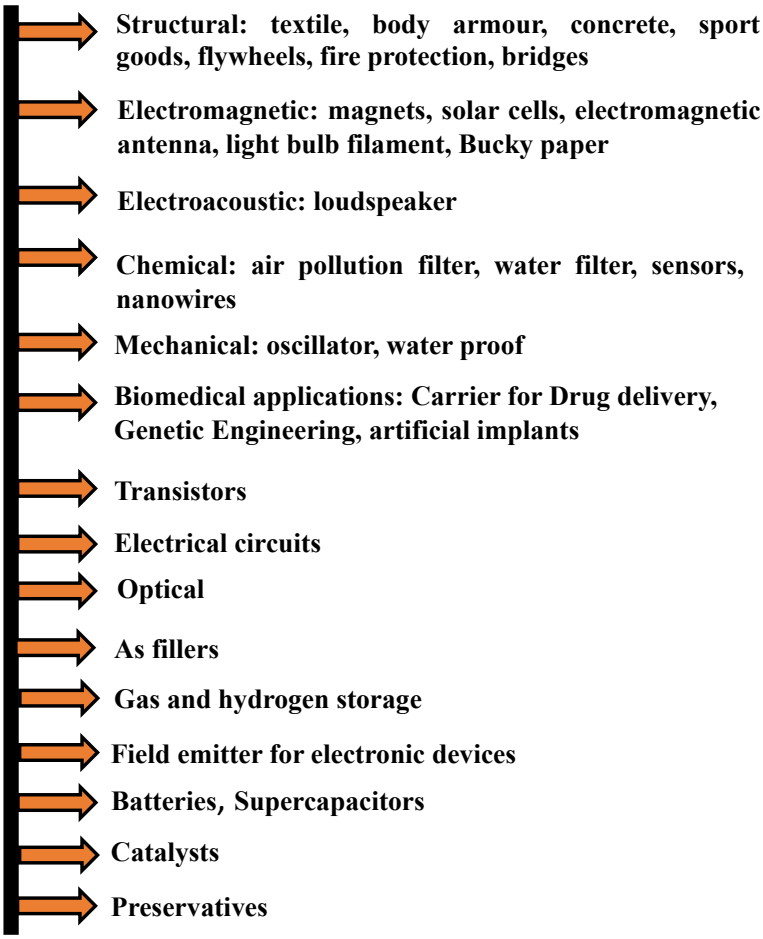

Fig. 6.15 Applications of CNTs

6.9 Challenges and Future Scope

6.9.1 Dispersion of Carbon Nanotubes

One of the major challenges associated with CNTs is they tend to agglomerate due to the weak intermolecular forces. This leads to considerable difficulties to disperse in a polymeric matrix and even in solvents. The disperse of CNTs can be improved for their possible dispersion inside a polymer matrix during the synthesis of polymer nanocomposites by functionalization of CNTs. Functionalization reduces the bundle formation and agglomeration of tubes of CNTs and ensures dispersion. Functionalization has also been an effective approach to purify CNTs as discussed earlier to enhance the degree of reactivity and homogeneous dispersion. The ollowing are the approaches taken to disperse the CNTs, either by covalent or non-covalent functionalization. The chemistry of functionalization has been included in Fig. 6.16.

Non-covalent functionalization includes hydrophobic and Pi–Pi interaction based on van der Waal's forces. This functionalization approach proves to be beneficial due to the nominal damage in CNT structure. Some common examples of non-covalent functionalization include the use of surfactants, protein interactions, and CNT wrapping [168]. In the case of covalent functionalization, the functional groups are attached to the tips and sidewalls of nanotubes. This functionalization leads to the change in nanotube structure permanently and irreversibly. Chemical entities such as carboxyl, fluorine, dichloro groups are added to the chain ends or surface of the nanotubes [120, 169, 170]. The main advantage of this functionalization is that here the nanotubes can be chemically bonded with the polymer matrix leading to the homogeneous dispersion of CNTs for the best possible utilization of unique features of CNTs. However, these types of functionalization may induce some defects in CNTs as well. Again, the dispersion of CNTs can also be improved by using

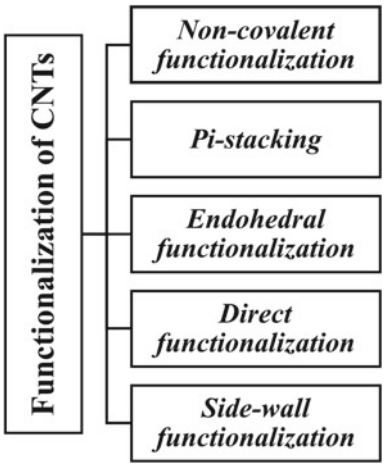

Fig. 6.16 Functionalization of CNTs. Drawn based on the concept taken from [168]

surfactants [171]. Some common surfactants are sodium dodecyl sulphate, dodecylbenzene sodium sulphonate, and polyethylene glycol. The Pi-stacking interaction of aromatic ring is responsible to promote adsorption of the surfactants. Again, in addition to benzene rings, the naphthenic groups also ensure a good affinity between surfactant and CNT.

6.9.2 Toxicity of Carbon Nanotubes

The immense potential of CNTs in different application areas opens up their importance in a number of industries. However, certain issues such as toxicity restrict their use. CNTs adversely affect human health specifically attacking the pulmonary systems a primary route of exposure [172]. Toxicity of CNTs and their adverse effect on human health is a serious issue, which is under the lens [173–176]. Hence, major initiatives are to be taken to resolve this issue. Overexposure of nanotubes leads to oxidative stress and inflammation as well [177]. Study reveals that the length and rigidity of CNTs have a renowned effect on pro-inflammation [178]. Further research is in need to explore the influence of nanotubes on physiochemical properties [179].

6.10 Concluding Remarks

This chapter elaborates the structure, properties, synthesis, purification, application aspects of the magical carbon nanomaterial, CNT. Research in worldwide is continued on various aspects of CNTs, such as synthesis of nanotubes of a particular diameter, precise control over its chirality, controlling the number of sidewalls of CNTs specifically for MWNTs, etc. Although the progress in this field is enormous, still these factors need to be addressed to optimize the synthesis of CNTs as per requirements. Again, in view of CNT growth, the synthesis of isolated nanotubes of similar diameter and chirality over the entire length of the nanotube is a big challenge. The detailed investigation into the growth parameters of CNTs will essentially provide valuable information in this respect. Finally, the large-scale synthesis of low-cost pure nanotubes of a particular structural parameter is definitely a future challenge to the research community.

Acknowledgements The authors acknowledge the financial support provided by the Department of Science and Technology, India, (DST/TMD/MES/2K16/37(G)) for carrying out this research work. Authors are thankful to Ms Tanvi Pal for drafting a figure.

References

1. G. Collin, in CFI. *Ceramic forum international* (Göller, 2000), pp. 28
2. J. Emsley, Astron. **31**, 87 (2003)
3. K.K. Kar, *Composite Materials* (Springer, Berlin, Heidelberg, 2017)
4. H.W. Kroto, J.R. Heath, S.C. O'Brien, R.F. Curl, R.E. Smalley, Nature **318**, 162 (1985)
5. D. Bethune, C.H. Kiang, M. De Vries, G. Gorman, R. Savoy, J. Vazquez, R. Beyers. Nature **363**, 605 (1993)
6. S. Iijima, T. Ichihashi, Nature **363**, 603 (1993)
7. A. Dasgupta, L.P. Rajukumar, C. Rotella, Y. Lei, M. Terrones, Nano Today **12**, 116 (2017)
8. K.K. Kar, J.K. Pandey, S. Rana, *Handbook of Polymer Nanocomposites. Processing, Performance and Application* (Springer Berlin Heidelberg, Berlin, Heidelberg, 2015)
9. J. Tersoff, R. Ruoff, Phys. Rev. Lett. **73**, 676 (1994)
10. N. Wang, Z.-K. Tang, G.-D. Li, J.S. Chen, Nature **408**, 50 (2000)
11. A.L. Kalamkarov, A. Georgiades, S. Rokkam, V.P. Veedu, M.N. Ghasemi-Nejhad, Int. J. Solids Struct. **43**, 6832 (2006)
12. R. Haddon Science **261**, 1545 (1993)
13. N. Hamada, S-i. Sawada, A. Oshiyama Phys. Rev. Lett. **68**, 1579 (1992)
14. A. Annu, B. Bhattacharya, P.K. Singh, P.K. Shukla, H.-W. Rhee, J. Alloys Compd. **691**, 970 (2017)
15. N.M. Rodriguez, A. Chambers, R.T.K. Baker, Langmuir **11**, 3862 (1995)
16. E. Ganesh, Inter. J. Innov. Technol. Explor. Eng. **2**, 311 (2013)
17. Q. Shi, Z. Yu, Y. Liu, H. Gong, H. Yin, W. Zhang, J. Liu, Y. Peng, Optics Commun. **285**, 4542 (2012)
18. X. Wu, X.C. Zeng, Nano Lett. **9**, 250 (2008)
19. S. Iijima, Nature **354**, 56 (1991)
20. P.J. Harris, S.C. Tsang, J.B. Claridge, M.L.H. Green, Chem Soc. Faraday Trans. **90**, 2799 (1994)
21. S. Zhu, G. Xu, Nanoscale **2**, 2538 (2010)
22. P. Agnihotri, S. Basu, K.K. Kar, Carbon **49**, 3098 (2011)
23. R. Sharma, K.K. Kar, Electrochim. Acta **156**, 199 (2015)
24. A. Huczko, Appl. Phys. A **74**, 617 (2002)
25. S. Fan, M.G. Chapline, N.R. Franklin, T.W. Tombler, A.M. Cassell, H. Dai, Science **283**, 512 (1999)
26. K. Hata, D.N. Futaba, K. Mizuno, T. Namai, M. Yumura, S. Iijima, Science **306**, 1362 (2004)
27. A. Bachtold, P. Hadley, T. Nakanishi, C. Dekker, Science **294**, 1317 (2001)
28. J. Kong, N.R. Franklin, C. Zhou, M.G. Chapline, S. Peng, K. Cho, H. Dai, Science **287**, 622 (2000)
29. J. Misewich, R. Martel, P. Avouris, J.C. Tsang, S. Heinze, J. Tersoff, Science **300**, 783 (2003)
30. S.J. Tans, A.R. Verschueren, C. Dekker, Nature **393**, 49 (1998)
31. M. Zhang, J. Li, Mater. Today **12**, (12) (2009)
32. S. Iijima, C. Brabec, A. Maiti, J. Bernholc, J. Chem. Phys. **104**, 2089 (1996)
33. B.I. Yakobson, C. Brabec, J. Bernholc, Phys. Rev. Lett. **76**, 2511 (1996)
34. M. Zhang, K.R. Atkinson, R.H. Baughman, Science **306**, 1358 (2004)
35. M. Zhang, S. Fang, A.A. Zakhidov, S.B. Lee, A.E. Aliev, C.D. Williams, K.R. Atkinson, R.H. Baughman, Science **309**, 1215 (2005)
36. L. Chernozatonskii, Phys. Lett. A **172**, 173 (1992)
37. G.E. Scuseria, Chem. Phys. Lett. **195**, 534 (1992)
38. V. Meunier, M.B. Nardelli, J. Bernholc, T. Zacharia, J.-C. Charlier, Appl. Phys. Lett. **81**, 5234 (2002)
39. G. Treboux, P. Lapstun, K. Silverbrook, Chem. Phys. Lett. **306**, 402 (1999)
40. A.N. Andriotis, M. Menon, D. Srivastava, L. Chernozatonskii, Appl. Phys. Lett. **79**, 266 (2001)

41. M. Menon, D. Srivastava, Phys. Rev. Lett. **79**, 4453 (1997)
42. V.N. Popov, Mater. Sci. Eng.: R: Reports **43**, 61 (2004)
43. D. Zhou, S. Seraphin, Chem. Phys. Lett. **238**, 286 (1995)
44. C. Luo, L. Liu, K. Jiang, L. Zhang, Q. Li, S. Fan, Carbon **46**, 440 (2008)
45. B. Satishkumar, P.J. Thomas, A. Govindaraj, C.N.R. Rao, Appl. Phys. Lett. **77**, 2530 (2000)
46. L.F. Su, J.N. Wang, F. Yu, Z.M. Sheng, Chem. Vap. Deposition **11**, 351 (2005)
47. D. Wei, Y. Liu, L. Cao, L. Fu, X. Li, Y. Wang, G. Yu, D. Zhu, Nano Lett. **6**, 186 (2006)
48. A. Ural, Y. Li, H. Dai, Appl. Phys. Lett. **81**, 3464 (2002)
49. S. Han, X. Liu, C. Zhou, J. Am. Chem. Soc. **127**, 5294 (2005)
50. S. Huang, X. Cai, J. Liu, J. Am. Chem. Soc. **125**, 5636 (2003)
51. J.F. AuBuchon, L.-H. Chen, A.I. Gapin, D.-W. Kim, C. Daraio, S. Jin, Nano Lett. **4**, 1781 (2004)
52. R. Gao, Z.L. Wang, S. Fan, J. Phys. Chem. B **104**, 1227 (2000)
53. W. Davis, R. Slawson, G. Rigby, Nature **171**, 756 (1953)
54. S. Amelinckx, X. Zhang, D. Bernaerts, X.F. Zhang, V. Ivanov, J.B. Nagy, Science **265**, 635 (1994)
55. M. Zhang, Y. Nakayama, L. Pan, Japn. J. Appl. Phys. **39**, L1242 (2000)
56. W. Wang, K. Yang, J. Gaillard, P.R. Bandaru, A.M. Rao, Adv. Mater. **20**, 179 (2008)
57. P. Bandaru, C. Daraio, K. Yang, A.M. Rao, J. Appl. Phys. **101**, 094307 (2007)
58. W.A. De Heer, P. Poncharal, C. Berger, J. Gezo, Z. Song, J. Bettini, D. Ugarte, Science **307**, 907 (2005)
59. Y. Nakayama, M. Zhang, Japn. J. Appl. Phys. **40**, L492 (2001)
60. C. Journet, W. Maser, P. Bernier, et al Nature **388**, 756 (1997)
61. L.P. Biró, C.A. Bernardo, G. Tibbetts, P. Lambin, *Carbon Filaments and Nanotubes: Common Origins, Differing Applications?* (Springer Science & Business Media, 2012)
62. H. Qiu, Z. Shi, L. Guan, L. You, M. Gao, S. Zhang, J. Qiu, Z. Gu, Carbon **44**, 516 (2006)
63. Y.-H. Wang, S.-C. Chiu, K.-M. Lin, Y.-Y. Li, Carbon **42**, 2535 (2004)
64. Z. Shi, Y. Lian, F.H. Liao, X. Zhou, Z. Gu, Y. Zhang, S. Iijima, H. Li, K.T. Yue, S-L. Zhang, J. Phys. Chem. Solids **61**, 1031 (2000)
65. K. Imasaka, Y. Kanatake, Y. Ohshiro, J. Suehiro, M. Hara, Thin Solid Films **506**, 250 (2006)
66. S.J. Lee, H.K. Baik, J-E. Yoo, J.H. Han, Diamond Relat. Mater. **11**, 914 (2002)
67. T. Guo, P. Nikolaev, A.G. Rinzler, D. Tomdnek, D.T. Colbert, R.E. Smalley, J. Phys. Chem. **99**, 10694 (1995)
68. J.H. Hafner, M.J. Bronikowski, B.R. Azamian, P. Nikolaev, A.G. Rinzler, D.T. Colbert, K.A. Smith, R.E. Smalley, Chem. Phys. Lett. **296**, 195 (1998)
69. H. Kataura, Y. Kumazawa, Y. Maniwa, Y. Ohtsuka, R. Sen, S. Suzuki, Y. Achiba, Carbon **38**, 1691 (2000)
70. M. Zhang, M. Yudasaka, S. Iijima, Chem. Phys. Lett. **336**, 196 (2001)
71. D. Nishide, H. Kataura, S. Suzuki, K. Tsukagoshi, Y. Aoyagi, Y. Achiba, Chem. Phys. Lett. **372**, 45 (2003)
72. M. Yudasaka, T. Komatsu, T. Ichihashi, Y. Achiba, S. Iijima, J. Phys. Chem. B **102**, 4892 (1998)
73. H. Zhang, Y. Ding, C. Wu, Y. Chen, Y. Zhu, Y. He, S. Zhong, Physica B: Conden. Matt. **325**, 224 (2003)
74. N. Braidy, M. El Khakani, G. Botton, Carbon **40**, 2835 (2002)
75. L.L. Lebel, B. Aissa, M.A. El Khakani, D. Therriault, Compos. Sci. Technol. **70**, 518 (2010)
76. K.B. Teo, C. Singh, M. Chhowalla, Encyclopedia of nanoscience and nanotechnology **10**, 1 (2003)
77. A. Szabó, C. Perri, A. Csató, G. Giordano, D. Vuono, J.B. Nagy, Materials **3**, 3092 (2010)
78. S.A. Steiner III, T.F. Baumann, B.C. Bayer, R. Blume, M.A. Worsley, W.J. MoberlyChan, E.L. Shaw, R. Schlög, A.J. Hart, S. Hofmann, B.L. Wardle, J. Am. Chem. Soc. **131**, 12144 (2009)
79. R. Smajda, J. Andresen, M. Duchamp, R. Meunier, S. Casimirius, K. Hernádi, L. Forró, A. Magrez, Physica status solidi (b) **246**, 2457 (2009)

80. H. Tempel, R. Joshi, J.J. Schneider, Mater. Chem. Phys. **121**, 178 (2010)
81. H.-R. Byon, H.-S. Lim, H.-J. Song, H.-C. Choi, Bull. Korean Chem. Soc. **28**, 2056 (2007)
82. Y. Xu, E. Dervishi, A.R. Biris, A.S. Biris, Mater. Lett. **65**, 1878 (2011)
83. D. Varshney, B.R. Weiner, G. Morell, Carbon **48**, 3353 (2010)
84. B. Brown, C.B. Parker, B.R. Stoner, J.T. Glass, Carbon **49**, 266 (2011)
85. H.D. Kim, J.-H. Lee, W.S. Choi, J. Korean Phys. Soc. **58**, 112 (2011)
86. O. Lee, J. Jung, S. Doo, S.-S. Kim, T.-H. Noh, K.-I. Kim, Y.-S. Lim, Metals Mater. Int. **16**, 663 (2010)
87. R. Sharma, S.-W. Chee, A. Herzing, R. Miranda, P. Rez, Nano Lett. **11**, 2464 (2011)
88. M. Palizdar, R. Ahgababazadeh, A. Mirhabibi, B. Alireza, P. Rik, P. Shima, J. Nanosci, Nanotechnol. **11**, 5345 (2011)
89. T. Tomie, S. Inoue, M. Kohno, Y. Matsumura, Diamond Relat. Mater. **19**, 1401 (2010)
90. Z. Yong, L. Fang, Z. Zhi-Hua, Micron **42**, 547 (2011)
91. A. Afolabi, A. Abdulkareem, S. Mhlanga, S.E. Iyuke, J. Exp. Nanosci. **6**, 248 (2011)
92. S. Dumpala, J.B. Jasinski, G.U. Sumanasekera, M.K. Sunkara, Carbon **49**, 2725 (2011)
93. J. Zhu, M. Yudasaka, S. Iijima, Chem. Phys. Lett. **380**, 496 (2003)
94. M. Paradise, T. Goswami, Mater. Des. **28**, 1477 (2007)
95. P. Nikolaev, M.J. Bronikowski, R.K. Bradley, F. Rohmund, D.T. Colbert, K.A. Smith, R.E. Smalley, Chem. Phys. Lett. **313**, 91 (1999)
96. Z. Tang, L. Zhang, N. Wang, X.X. Zhang, G.H. Wen, G.D. Li, J.N. Wang, C.T. Chan, P. Sheng, Science **292**, 2462 (2001)
97. D. Resasco, W. Alvarez, F. Pompeo, L. Balzano, J.E. Herrera, B. Kitiyanan, A. Borgna, J. Nanopart. Res. **4**, 131 (2002)
98. W. Hsu, J. Hare, M. Terrones, H.W. Kroto, D.R.M. Walton, P.J.F. Harris, Nature **377**, 687 (1995)
99. J. Bai, A.-L. Hamon, A. Marraud, B. Jouffrey, V. Zymla, Chem. Phys. Lett. **365**, 184 (2002)
100. D. Laplaze, P. Bernier, W. Maser, G. Flamant, T. Guillard, A. Loiseau, Carbon **36**, 685 (1998)
101. D. Luxembourg, G. Flamant, D. Laplaze, Carbon **43**, 2302 (2005)
102. Y. Gogotsi, J.A. Libera, M. Yoshimura, J. Mater. Res. **15**, 2591 (2000)
103. Y. Gogotsi, N. Naguib, J. Libera, Chem. Phys. Lett. **365**, 354 (2002)
104. V. Jourdain, H. Kanzow, M. Castignolles, A. Loiseau, P. Bernier, Chem. Phys. Lett. **364**, 27 (2002)
105. F. Ding, K. Bolton, A. Rosen, J. Phys. Chem. B **108**, 17369 (2004)
106. B.K. Kaushik, M.K. Majumder, Carbon nanotube: Properties and applications, in *Carbon Nanotube Based VLSI Interconnects* (Springer, 2015)
107. S. Patole, P. Alegaonkar, H-C. Lee, J-B. Yoo, Carbon **46**, 1987 (2008)
108. J. Prasek, J. Drbohlavova, J. Chomoucka, J. Hubalek, O. Jasek, V. Adam, R. Kizek, J. Mater. Chem. **21**, 15872 (2011)
109. N. Muradov, Int. J. Hydrogen Energy **26**, 1165 (2001)
110. J. Pinilla, R. Moliner, I. Suelves, M.J. Lázaro, Y. Echegoyen, J.M. Palacios, Int. J. Hydrogen Energy **32**, 4821 (2007)
111. N. Fotopoulos, J. Xanthakis, Diamond Relat. Mater. **19**, 557 (2010)
112. S. Naha, I.K. Puri, J. Phys. D Appl. Phys. **41**, 065304 (2008)
113. G. Hajime, F. Terumi, F. Yoshiya, O. Toshiyuki, *Method of purifying single wall carbon nanotubes from metal catalyst impurities* (Honda Giken Kogyo Kabushiki Kaisha, Japan, 2002)
114. E. Borowiak-Palen, T. Pichler, X. Liu, M. Knupfer, A. Graff, O. Jost, W. Pompe, R.J. Kalenczuk, J. Fink, Chem. Phys. Lett. **363**, 567 (2002)
115. S. Bandow, A. Rao, K. Williams, A. Thess, R.E. Smalley, P.C. Eklund, J. Phys. Chem. B **101**, 8839 (1997)
116. V. Georgakilas, D. Voulgaris, E. Vazquez, M. Prato, D.M. Guldi, A. Kukovecz, H. Kuzmany, J. Am. Chem. Soc. **124**, 14318 (2002)
117. H. Kajiura, S. Tsutsui, H. Huang, Y. Murakami, Chem. Phys. Lett. **364**, 586 (2002)
118. L. Thiên-Nga, K. Hernadi, E. Ljubović, S. Garaj, L. Forró, Nano Lett. **2**, 1349 (2002)

119. S. Niyogi, H. Hu, M. Hamon, P. Bhowmik, B. Zhao, S.M. Rozenzhak, J. Chen, M.E. Itkis, M.S. Meier, R.C. Haddon, J. Am. Chem. Soc. **123**, 733 (2001)
120. H-C. Wu, X. Chang, L. Liu, F. Zhaoa, Y. Zhao, J. Mater. Chem. **20**, 1036 (2010)
121. P.G. Collins, P. Avouris, Sci. Am. **283**, 62 (2000)
122. T.W. Ebbesen, H.J. Lezec, H. Hiura, J.W. Bennett, H.F. Ghaemi, T. Thio, Nature **382**, 54 (1996)
123. B.Q. Wei, R. Vajtai, P.M. Ajayan, Appl. Phys. Lett. **79**, 1172 (2001)
124. J.C. Stallard, W. Tan, F.R. Smail, T.S. Gspann, A.M. Boies, N.A. Fleck, Extreme Mechanics Lett. **21**, 65 (2018)
125. S. Sakurai, F. Kamada, D.N. Futaba, M. Yumura, K. Hata, Nanoscale Res. Lett. **8**, 546 (2013)
126. L. Hu, D.S. Hecht, G. Gruner, Nano Lett. **4**, 2513 (2004)
127. E. Bekyarova, M.E. Itkis, N. Cabrera, B. Zhao, A. Yu, J. Gao, R.C. Haddon, J. Am. Chem. Soc. **127**, 5990 (2005)
128. H.E. Unalan, G. Fanchini, A. Kanwal, A.D. Pasquier, M. Chhowalla, Nano Lett. **6**, 677 (2006)
129. Z.R. Li, H.R. Kandel, E. Dervishi, V. Saini, Y. Xu, A.R. Biris, D. Lupu, G.J. Salamo, Langmuir **24**, 2655 (2008)
130. G. Gruner, J. Mater. Chem. **16**, 3533 (2006)
131. X. Wang, Q. Jiang, W. Xu, W. Cai, Y. Inoue, Y. Zhu, Carbon **53**, 145 (2013)
132. S. Frankland, A. Caglar, D. Brenner, M. Griebel, J. Phys. Chem. B **106**, 3046 (2002)
133. M.F. Yu, J. Eng. Mater. Technol. **126**, 271 (2004)
134. B.T. Kelly, *Physics of Graphite* (Applied Science, London, 1981)
135. X. Lei, T. Natsuki, J. Shi, Q.-Q. Ni, J. Nanomater. **2011**, 1 (2011)
136. G. Overney, W. Zhong, D. Tom´anek, Zeitschrift f˙ur Physik D **27**, 93 (1993)
137. J.P. Lu, J. Phys. Chem. Solids **58**, 1649 (1997)
138. B.I. Yakobson, J. Electrochem. Soc. **97–42**, 549 (1997)
139. A.M. Fennimore, T.D. Yuzvinsky, W.Q. Han, M.S. Fuhrer, J. Cumings, A. Zettl, Nature **424**, 408 (2004)
140. P.A. Williams, S.J. Papadakis, A.M. Patel, M.R. Falvo, S. Washburn, R. Superfine, Phys. Rev. Lett. **89**, 255502 (2002)
141. C. Velasco-Santos, A.L. Martinez-Hernandez, F.T. Fisher, R. Ruoff, V.M. Castaño, Chem. Mater. **15**, 4470 (2003)
142. R.J. Chen, H.C. Choi, S. Bangsaruntip, E. Yenilmez, X. Tang, Q. Wang, Y.-L. Chang, H. Dai, J. Am. Chem. Soc. **126**, 1563 (2004)
143. E. Pop, D. Mann, Q. Wang, K. Goodson, H. Dai, Nano Lett. **6**, 96 (2006)
144. P. Kim, L. Shi, A. Majumdar, P.L. McEuen, Phys. Rev. Lett. **87**, 215502/1–4 (2001)
145. H. Xie, A. Cai, X. Wang, Phys. Lett. A **369**, 120 (2007)
146. M.A. Stroscio, M. Dutta, D. Kahn, K.W. Kim, Superlattices Microstruct. **29**, 405 (2001)
147. M. Grujicic, G. Cao, B. Gersten, Mater. Sci. Eng., B **107**, 204 (2004)
148. J. Maultzsch, S. Reich, C. Thomsen, E. Dobardžić, I. Milošević, M. Damnjanović, Solid State Commun. **121**, 471 (2002)
149. H. Ishii, N. Kobayashi, K. Hirose, Physica E **40**, 249 (2007)
150. A. Kasuya, Y. Saito, Y. Sasaki, M. Fukushima, T. Maedaa, C. Horie, Y. Nishina, Mater. Sci. Eng. A **217/218**, 46 (1996)
151. V.N. Popov, Carbon **42**, 991 (2004)
152. J.L. Sauvajol, E. Anglaret, S. Rols, L. Alvarez, Carbon **40**, 1697 (2002)
153. J. Hone, M. Whitney, C. Piskoti, A. Zettl, Phys. Rev. B **59**, R2514 (1999)
154. J. Hone, M. Whitney, A. Zettl, Synth. Met. **103**, 2498 (1999)
155. A. Cummings, M. Osman, D. Srivastava, M. Menon, Phys. Rev. B **70**, 115405/1–6 (2004)
156. F.Y. Meng, S. Ogata, D.S. Xu, Y. Shibutani, S.Q. Shi, Phys. Rev. B **75**, 205403/1–6 (2007)
157. M.A. Osman, D. Srivastava, Nanotechnol. **12**, 21 (2001)
158. A. Helland, P. Wick, A. Koehler, K. Schmid, C. Som, Environ. Health Perspect. **115**, 1125 (2007)
159. R.H. Baughman, A.A. Zakhidov, W.A. De Heer, Science **297**, 787 (2002)

160. A. Cao, H. Zhu, X. Zhang, X. Li, D. Ruan, C. Xu, B. Wei, J. Liang, D. Wu, Chem. Phys. Lett. **342**, 510 (2001)
161. C. Jayesh, K.K. Kar, J. Mater. Chem. A **4**, 9910 (2016)
162. S.K. Singh, P. Azad, M.J. Akhtar, K.K. Kar, A.C.S. Appl, Nano Mater. **9**, 94746 (2018)
163. C. Jayesh, K.K. Kar, RSC Adv. **5**, 34335 (2015)
164. R. Sharma, K.K. Kar, Mater. Lett. **137**, 150 (2014)
165. J. Cherusseri, R. Sharma, K.K. Kar, Carbon **105**, 113 (2016)
166. R. Sharma, A.K. Yadav, V. Panwar, K.K. Kar, J. Reinforced Plast. Compos. **34**, 941 (2015)
167. S. Kar, R. Bindal, S. Prabhakar, P.K. Tewari, K. Dasgupta, D. Sathiyamoorthy, Int. J. Nuclear Desalination **3**, 143 (2008)
168. A. Hirsch, Angew. Chem. Int. Ed. **41**, 1853 (2002)
169. J.-H. Kim, B.-G. Min, Carbon lett. **11**, 298 (2010)
170. K.J. Saeed, Chem. Soc. Pak. **32**, 559 (2010)
171. H. Wang, Current Opinion in Colloid Interface Sci **14**, 364 (2009)
172. B. Satishkumar, A. Govindaraj, M. Nath, C.N.R. Rao, J. Mater. Chem. **10**, 2115 (2000)
173. Y.-M. Choi, D.-S. Lee, R. Czerw, P.-W. Chiu, N. Grobert, M. Terrones, M. Reyes-Reyes, H. Terrones, J.-C. Charlier, P.M. Ajayan, S. Roth, D.L. Carroll, Y.-W. Park, Nano Lett. **3**, 839 (2003)
174. G. Oberdörster, J. Internal, Medicine **267**, 89 (2010)
175. A.A. Shvedova, V.E. Kagan, B. Fadeel, Annu. Rev. Pharmacool. Toxicol. **50**, 63 (2010)
176. P.P. Simeonova, Nanomedicine **4**, 373 (2009)
177. A. Nemmar, H. Vanbilloen, M. Hoylaerts, P.H. Hoet, A. Verbruggen, B. Nemery, American J. Respiratory. Crit. Care Med. **164**, 1665 (2001)
178. C.A. Poland, R. Duffin, I. Kinloch, A. Maynard, W.A.H. Wallace, A. Seaton, V. Stone, S. Brown, W. MacNee, K. Donaldson, Nature Nanotechnol. **3**, 423 (2008)
179. C-W. Lam, J.T. James, R. McCluskey, S. Arepalli, R.L. Hunter, Crit. Rev. Toxicol. **36**, 189 (2006)